ISSN 0036-0244, Russian Journal of Physical Chemistry A, 2019, Vol. 93, No. 2, pp. 338–342. © Pleiades Publishing, Ltd., 2019.
Russian Text © R.Kh. Dzhanabekova, E.V. Seliverstova, A.Zh. Zhumabekov, N.Kh. Ibrayev, 2019, published in Zhurnal Fizicheskoi Khimii, 2019, Vol. 93, No. 2, pp. 284–289.

PHYSICAL CHEMISTRY
OF SURFACE PHENOMENA

Fabricating and Examining of Langmuir Films of Reduced Graphene Oxide

R. Kh. Dzhanabekova[a], E. V. Seliverstova[a,*], A. Zh. Zhumabekov[a], and N. Kh. Ibrayev[a,]**

[a] *Institute of Molecular Nanophotonics, Buketov Karaganda State University, Karaganda, 100028 Kazakhstan*

**e-mail: genia_sv@mail.ru*

***e-mail: niazibrayev@mail.ru*

Received April 4, 2018

Abstract—The effect the transfer pressure has on structural, optical, and electrophysical properties of Langmuir-Blodgett (LB) films of reduced graphene oxide (rGO) is studied. Investigation of physicochemical properties of rGO monolayers on the subphase surface shows that the rGO monolayer on the subphase surface predominantly exists in the liquid state. Increased surface pressure in the film makes rGO particles lie closer to and contact one another, followed by the overlapping and crumpling of some film sheets. Electron microscope studies show that as monolayers are transferred onto solid substrates, rGO forms uniform island-type films with clearly discernible clusters whose density grows along with surface pressure. The synthesized rGO films are highly transparent (87–96%) in the visible spectral region. The LB films transferred onto solid substrates at a lower surface pressure exhibit the best electrophysical and electroconductive properties. The reported findings can be used in developing technology for synthesizing transparent nanosized films from reduced graphene oxide and its derivatives for use in molecular electronics and photovoltaics.

Keywords: Langmuir–Blodgett films, reduced graphene oxide, transfer pressure, structure, optical properties, electrophysical properties

DOI: 10.1134/S0036024419020092

INTRODUCTION

As with other nanostructures, the properties of graphene and its modified derivatives depend on their dimensions and morphology. 2D graphene exhibits quite different properties than those of its 1D form (i.e., carbon nanotubes). The 2D structure of graphene makes it compatible with planar substrates, which can be a viable alternative for replacing silicon. In addition, the 2D structure and atomic dimensions of graphene layers impart unique properties to them [1]. High electrical conductivity and high ratios between surface area and volume are the most prominent characteristics of layered graphene nanostructures [2]. It was also demonstrated in [1, 3] that graphene has a high specific surface area, high electron mobility, and a higher oxidative potential than Pt, the material normally used in dye-sensitized solar cells. Due to the diversity of the existing forms of graphene, we can improve the required parameters of solar cell electrodes. For example, reduced graphene oxide (rGO) has surface lattice imperfections, meaning that it exhibits stronger catalytic activity than fully reduced, defect-free graphene [4, 5]. This makes it more promising for use as a conducting layer in different elements of molecular electronics and photovoltaics. It therefore make sense to investigate the conditions for fabricating solid rGO films with desired properties.

The Langmuir–Blodgett (LB) technique can be used to deposit consecutive rGO layers and thus control film thickness. We can thus control film transparence, conductivity, and resistance, making Langmuir graphene films with optimized optoelectronic properties promising materials for use in nanodevices and solar cells. Despite the popularity of graphene and graphene-based films, there are few works on the effect different conditions of fabricating graphene films using the LB technique have on their properties.

In this work, we investigated the conditions for creating stable monolayers and fabricating thin solid rGO-based films using the LB technique, as along with the effect these conditions have on the structural, optical, and electrophysical properties of solid LB films.

EXPERIMENTAL

Dispersions of reduced graphene oxide (rGO, Sigma Aldrich) in chloroform were used in this work. Prior to use, chloroform of pure for analysis grade was purified via shaking with H_2SO_4, dried over calcium chloride, and distilled. To prepare the rGO dispersion, 1 mL of the solvent was added to 1 mg of rGO,

and the resulting dispersed system was held in an ultrasonic bath for 20 min. The solution was then placed into a laboratory centrifuge for 1 h and spun at a speed of 3800 rpm. The decantate was used to produce Langmuir films. The quality of the dispersion was evaluated according to the size distribution of graphene particles in the solution using a Zetasizer nano system (Malvern). The measurements showed that the average size of rGO particles prior to ultrasonic treatment was 1200 nm. After 10 min of dispersion, the particle size were ranged between 200 and 300 nm. Particles 300 nm in size were predominantly observed (~45%), followed by particles 250 and 220 nm in diameter (~30% each). Further dispersion of particles in the solution for 40 min produced negligible changes in particle size.

The monolayers to be analyzed were formed at the water–air interface by spreading the solution in a Langmuir–Blodgett trough (KSV NIMA Medium). Deionized water, purified using an AquaMax water purification system, was used as the subphase. The water's specific resistance was 18.2 MΩ/cm. The water's surface tension was 72.8 mN/m at pH 5.6 and a temperature of 22°C. The rGO monolayers were transferred to solid substrates using the LB technique with a vertical lifting procedure at different surface pressures (π) of 10, 20, and 34 mN/m. Film thickness was equal to one Z-type transferred monolayer (the substrate moved upward through the monolayer). Monolayers were compressed at a barrier speed of 5 mm/min; the substrate speed was 2 mm/min and the time of monolayer stabilization was 30 min. Quartz glasses and FTO-coated glass substrates were used. The estimated film transfer coefficient during monolayer transfer was almost 1.

The morphology of rGO films on surfaces of FTO-coated glasses was studied on a TESCAN Mira-3 scanning electron microscope. The optical properties of the films were investigated using a Cary-300 spectrophotometer (Agilent).

When studying the effect transfer pressure had on the electrophysical properties of reduced graphene oxide films, measurements were made on a J-30 potentiostat-galvanostat (Elins, Russia). The samples were illuminated with a 100 mW/cm^2 xenon lamp. Photogenerated current was recorded in the steady-state mode at zero bias potential. The applied signal amplitude was 25 mV; the frequency was scanned in the range from 1 MHz to 100 mHz. Iodolyte H30 (Solaronix, Switzerland) was used as an electrolyte. Pt film deposited electrochemically from an aqueous solution of H_2PtCl_6 (10 mM) and KCl (10 mM) was used as the reference sample [6].

The catalytic activity of rGO films was measured using a potentiostat (Elins, Russia) and a standard three-electrode cell. Platinum foil was used as an auxiliary electrode and AgCl as the reference electrode. The measurements were made in 0.1 M NaOH electrolyte. When measuring the photo-generated current, the film surface was illuminated with modulated intensity light from a 35 mW/cm^2 xenon lamp.

RESULTS AND DISCUSSION

To study the conditions under which stable rGO monolayers form, we applied 25 μL of rGO dispersion onto a subphase surface. Measurements showed that a smaller amount of the investigated substance yielded a nonuniform monolayer. The recorded π–*A* isotherms (Fig. 1a) revealed that the behavior of rGO monolayers differs noticeably from that of single-layer graphene oxide (SLGO) and nitrogen-doped graphene oxide (NGO) Langmuir films [7, 8].

A very short gaseous phase (at pressures up to ~1 mN/m) was observed in rGO films even for the minimum amount of the applied substance. An expanded liquid phase [9] was observed in the 1 to 20 mN/m range of pressures. At pressures above 20 mN/m, the monolayers transformed into the liquid-condensed phase. The obvious monolayer collapse typical of surfactants was not observed. At pressures above 40 mN/m, however, the isotherm curve changed its slope, demonstrating that the structure of the Langmuir film had been altered. We could see monolayer folds near the barriers on the subphase surface.

We next studied the stability of rGO monolayers by monitoring the evolution of surface pressure and monolayer area at a constant surface pressure π for 30 min [10]. The following π values were selected: 10 and 20 mN/m for the liquid-expanded monolayer phase, and 38 and 50 mN/m corresponding to different densities of the liquid-condensed phase. The Langmuir films were spread from the rGO dispersion in chloroform onto the surface of the aqueous subphase. Prior to compression, the films were kept for at least 30 min to let the solvent completely evaporate and the monolayer stabilize. The results showed that at π = 10 and 20 mN/m, the preset surface pressure fell slightly over time by 0.01–0.02 mN/m, and the monolayer surface was reduced by 15 and 14 cm^2, respectively. At 38 mN/m, there was a deviation from the preset π value by 0.05 mN/m. After monitoring for 13 min, the surface pressure changed by ~0.2 mN/m. The monolayer surface was reduced by 3.2 cm^2 in 30 min. At 50 mN/m, the surface pressure fell by 0.5 mN/m in 7 min, and the monolayer shrank by 3.2 cm^2.

We can therefore see that the rGO monolayer was unstable at a pressure of 50 mN/m. The small fluctuations in surface pressure over time that were recorded at π = 10, 20, and 38 mN/m indicate that rGO particles exist in thermodynamic equilibrium with the subphase and the microenvironment.

The stability of rGO monolayers at the water–air interface was also studied by measuring the compression/decompression curves of the monolayers up to a certain π value and after repeated film compression

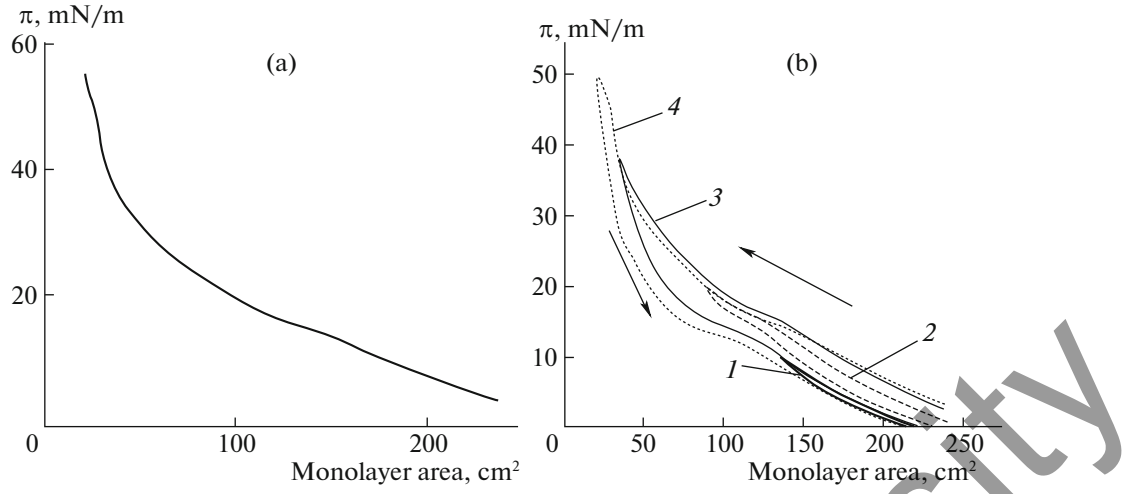

Fig. 1. (a) Compression isotherms of rGO monolayers on the subphase surface and (b) curves of the compression hysteresis of rGO monolayers until different surface pressures are reached: (*1*) 10, (*2*) 20, (*3*) 38, and (*4*) 50 mN/m.

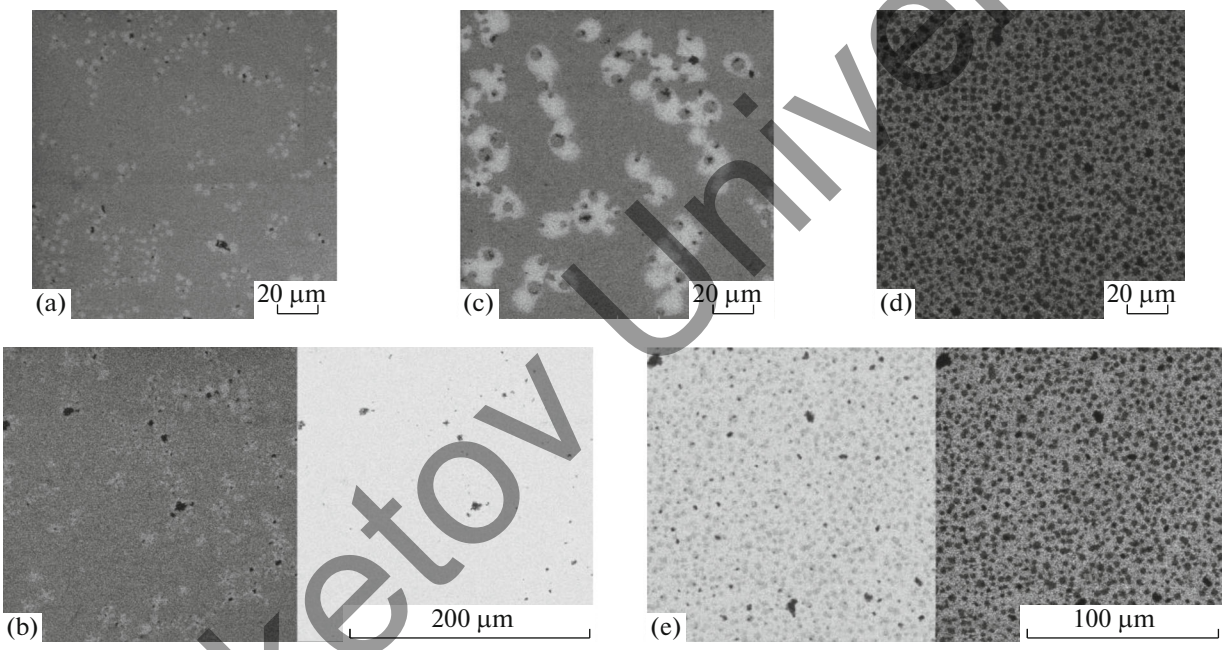

Fig. 2. SEM images of the rGO LB film transferred at different surface pressures: (a, b) 10, (c) 20, and (d, e) 35 mN/m. Images (b, e) were recorded using BSE and SE detectors.

(Fig. 1b). To record all of the curves, equal volumes of the solution (20 μL) were applied onto the subphase surface. We can see in Fig. 1b that the smallest changes in film surface area occurred after it was compressed to a pressure of 10 mN/m (curve *1*). Changes in the area of the monolayer were greatest after the films were compressed to pressures of 38 and 50 mN/m, and the monolayer began to exist in the liquid-condensed state [9].

These findings indicate that rGO particles lie quite far away from one another as the film is initially compressed and return to their original positions after monolayer decompression. As the surface pressure increases, the particles approach one another and come into contact as demonstrated in [11, 12]. It is likely that this is accompanied by the overlapping and crumpling of some sheets of reduced graphene oxide. Such interaction between rGO particles is reversible, since the recorded curves of repeated monolayer compression to pressures of 10, 20, and 38 mN/m overlap each other.

The multiple compression curves recorded for rGO differ from the data obtained for NGO and SLGO, where repeated compression reduced the film surfaces; due to the removal and reduction of oxygen-containing moieties in their structure, rGO particles were more hydrophobic [12, 13] than those of NGO and SLGO. Their interactions are mostly a result of

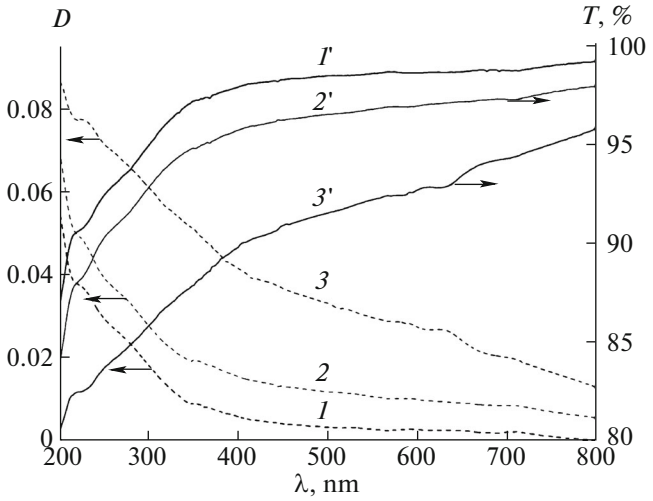

Fig. 3. Absorption (curves *1*, *2*, and *3*) and transmission spectra (curves *1'*, *2'*, and *3'*) of rGO LB films synthesized at different pressures: (*1*, *1'*) 10, (*2*, *2'*) 20, and (*3*, *3'*) 35 mN/m.

the ππ* conjugation of intact graphene layers, which requires considerable overlapping and the superimposition of particles.

The SEM images of the LB reduced graphene oxide films were recorded. Measurements showed that uniform island-type films with clearly discernible clusters formed on the solid rGO substrates (Fig. 2). When using a backscattered electron detector for a film fabricated at $\pi = 10$ mN/m, the SEM images contained almost no regions with a multilayered structure (Fig. 2d).

Cluster density rose as surface pressure increased (Figs. 2c and 2d). The film structure was formed by particles 2–4 μm in diameter. The surface between these microparticles was also occupied by rGO particles. The density of multilayered structures grew in films synthesized at 35 mN/m. Analysis of the SEM images and the hysteresis data thus showed that monolayer compression makes rGO particles lie closer to one another. This results in the superimpositioning of particles and the formation of multilayered particles within a monolayer, rather than in crumpling and the formation of wrinkles and folds, as was suggested above.

Next we studied the effect of the transfer pressure on the optical properties of rGO LB films. The absorption spectra of rGO films contain a broad band with a maximum at 230 nm and a poorly expressed shoulder at 270 nm (Fig. 3). The absorption band at 230 nm is known to be formed by ππ* transitions between orbitals in aromatic C–C bonds, while the shoulder at 300 nm is associated with the $n \rightarrow \pi^*$ transitions in C=O bonds [12].

We can see from curves *1* and *2* that doubling the pressure of monolayer transfer increased the optical density of the film by 60%. For the film produced at 35 mN/m, the absorbance of the sample at the absorption band of graphene grew by another 65%. As with SLGO films [14, 15], the reduced graphene oxide films were transparent in the 400 to 800 nm range of wavelengths. The film fabricated at 10 mN/m was thus characterized by the highest transparence (*T* fluctuated from 97 to 99%, curve *1'*). The coating deposited at 35 mN/m transmitted 88–95% of the incident light. These figures are higher than those for the SLGO [7, 14] and NGO [8] films that we obtained earlier.

In studying the electrophysical and electrotransport properties of reduced graphene oxide LB films, we plotted their impedance spectra (Fig. 4).

The impedance spectra obtained for the films were used to calculate the effective rate k_{eff} of recombination, effective electron lifetime τ_{eff}, electron transport resistance R_w in the graphene oxide film, and charge transfer resistance R_k associated with electron recombination [16, 17] (Table 1). The results showed that the film deposited at a pressure of 10 μN/m had the best electrotransport properties. It was characterized by minimal electron transport resistance and a shorter

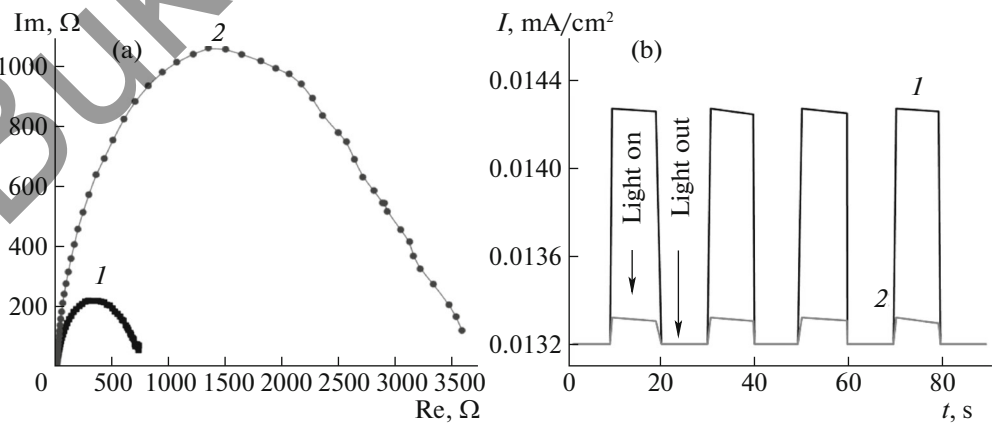

Fig. 4. (a) Impedance spectrum of films and (b) photo-induced current in rGO films deposited at different pressures of (*1*) 10 and (*2*) 35 mN/m.

Table 1. Electrophysical parameters of different electrodes

Sample	k_{eff}, s^{-1}	τ_{eff}, s	R_k, Ω	R_w, Ω
Pt	4000	0.00025	17	26
10 mN/m rGO	93	0.01	723	21
35 mN/m rGO	21	0.047	3570	25

effective electron lifetime (0.01 s). In all films, electron transport resistance varied from 21 to 25 Ω. This figure is consistent with the values reported in [18] for graphene film. Most electrons return to the electrolyte without participating in the passage of current through a film [18], though the lifetime of electron diffusion in graphene oxide LB films is an order of magnitude longer than in Pt films. The high resistance to charge carrier transfer in graphene oxide LB films could be due to there being no good contact between individual graphene oxide particles on the FTO surface, as was verified by the SEM data.

Thomas et al. [16] believed that R_k is the key parameter of the photocatalytic activity of nanostructures. The lower resistance R_k, the higher the photocatalytic activity. For the rGO film deposited at a pressure of 10 mN/m, electron transport resistance R_k was thus ~700 Ω, barely one-fifth of the values for the films deposited at 35 mN/m. The resulting data show that the electrotransport characteristics of rGO LB films depend strongly on the conditions of fabrication.

Figure 4b shows that the highest photo-generated current density was induced by irradiating the rGO films deposited at 10 mN/m. The films transferred at 35 mN/m generate current several times less efficiently, due possibly to their having a nonordered structure without sufficient contact between the reduced graphene oxide particles. The SEM images thus show that particles are quite far away from each other at a transfer pressure of 10 mN/m. In the films transferred at 35 mN/m, particles overlap each other to produce multi-layered clusters and increase the resistance in the film.

CONCLUSIONS

Our measurements show that the structural, optical, and electrophysical properties of reduced graphene oxide LB films can be altered by varying particle density within a monolayer as the monolayer is transferred to solid substrates.

It was demonstrated that when monolayers are transferred to solid substrates, rGO forms uniform island-type films with clearly discernible clusters whose density grows along with surface pressure. The absorption spectrum of LB films contained a band in the UV region with a maximum at 230 nm. Increasing the surface pressure of monolayer transfer onto a solid substrate did not alter the shape of the absorption band but doubled the optical density of the absorption band of reduced graphene oxide. The synthesized rGO films were characterized by high transparency (87–96%) in the visible spectral region. The rGO LB films synthesized at a transfer pressure of 10 mN/m had the best electrophysical and electrical conductivity parameters.

ACKNOWLEDGMENTS

This work was supported by the Ministry of Education and Science of the Republic of Kazakhstan, project nos. AP05132443 and BR05236691.

REFERENCES

1. C. X. Guo, G. H. Guai, and C. M. Li, Adv. Energy Mater. **1**, 448 (2011).
2. M. He, J. Jaehan, and Q. Feng, J. Mater. Chem. **22**, 24254 (2012).
3. J. D. Roy-Mayhew, D. J. Bozym, C. Punckt, and I. A. Aksay, ACS Nano **4**, 6203 (2010).
4. R. Whitby, V. M. Gun'ko, A. Korobeinyk, R. Busquets, et al., ACS Nano **6**, 3967 (2012).
5. R. L. D. Whitby, A. Korobeinyk, V. M. Gun'ko, D. B. Wright, et al., J. Phys. Chem. C, No. 117, 11829 (2013).
6. B. O'Regan and M. Gratzel, Nature (London, U.K.) **353**, 737 (1991).
7. E. Seliverstova, N. Kh. Ibrayev, and R. Kh. Dzhanabekova, Russ. J. Phys. Chem. A **91**, 1761 (2017).
8. R. Kh. Dzhanabekova, E. V. Seliverstova, and N. Kh. Ibrayev, Bull. Karaganda Univ., Phys. Ser., No. 1 (85), 8 (2017).
9. A. W. Adamson, *Physical Chemistry of Surfaces* (Wiley, New York, 1990).
10. V. V. Arslanov, Russ. Chem. Rev. **69**, 883 (2000).
11. Q. Zheng, W. H. Ip, X. Lin, N. Yousefi, et al., ACS Nano **5**, 6039 (2011).
12. L. Xiaolin, Z. Guangyu, B. Xuedong, S. Xiaoming, et al., Nat. Nanotechnol. **3**, 538 (2008).
13. D. S. Sutar, K. Narayanam Pavan, G. Singh, et al., Thin Solid Films **520**, 5991 (2012).
14. E. V. Seliverstova, N. Kh. Ibrayev, and R. Kh. Dzhanabekova, Nanosyst.: Phys., Chem., Mat., No. 7 (1), 65 (2016).
15. E. Seliverstova, N. Ibrayev, R. Dzhanabekova, and V. Gladkova, IOP Conf. Ser.: Mater. Sci. Eng. **110**, 1 (2016).
16. S. Thomas, T. G. Deepak, G. S. Anjusree, T. A. Arun, et al., J. Mat. Chem., No. 13, 1 (2014).
17. M. Adachi, M. Sakamoto, J. Jiu, Yu. Ogata, et al., J. Phys. Chem. **110**, 13872 (2006).
18. R. Cruz, D. Pacheco Tanaka, and A. Mendes, Solar Energy **86**, 716 (2012).

Translated by D. Terpilovskaya